PHILOSOPHICAL TRANSACTIONS OF THE ROYAL SOCIETY A MATHEMATICAL, PHYSICAL & ENGINEERING SCIENCES

The Flow of Air and of an Inviscid Fluid around an Elliptic Cylinder and an Aerofoil of Infinite Span, Especially in the Region of the Forward Stagnation Point

A. Fage

Phil. Trans. R. Soc. Lond. A 1928 **227**, 1-19
doi: 10.1098/rsta.1928.0001

PHILOSOPHICAL TRANSACTIONS.

I. *The Flow of Air and of an Inviscid Fluid around an Elliptic Cylinder and an Aerofoil of Infinite Span, especially in the Region of the Forward Stagnation Point.*

By A. Fage, *A.R.C.Sc., of the Aerodynamics Department, National Physical Laboratory.*

(*Communicated by* L. Bairstow, *F.R.S.*)

(Received January 4, 1927—Read February 17, 1927.)

Introduction.

(1) A study of some of the characteristics of the two-dimensional flow around an aerofoil mounted in a wind tunnel has been made by L. W. Bryant and D. H. Williams.* This work included measurements of velocity in the neighbourhood of the aerofoil, and showed that under certain conditions the theoretical law of Kutta and Joukowski† can be applied in practice to an aerofoil. The flow pattern measured in the wind tunnel was also compared with that for an inviscid flow having an equal circulation. The purpose of the present paper‡ is to examine, in detail, the relationship between the inviscid and the wind-tunnel flows at the nose of an elliptic cylinder and also of an aerofoil of infinite span.

Throughout the paper the term circulation is used in the usual hydrodynamic sense, it being understood that for a wind-tunnel flow the contour is not taken too close to the boundary of the body.§ Attention has been focussed on the forward stagnation point, because it is a well-defined point on the surface where the pressure is a maximum.

(2) The investigation consists of three parts. In the first, experiments made with an elliptic cylinder of large eccentricity (0·9657) are analysed. This model has been selected because the position of the stagnation point for an inviscid flow can be determined

* "An Investigation of the Flow of Air around an Aerofoil of Infinite Span." With an Appendix by Professor G. I. Taylor, "A Note on the Relation between the Lift of an Aerofoil and the Circulation Around it." 'Phil. Trans. Roy. Soc.,' Series A, vol. 225.

† This law states that the lift per unit span is equal to the product of the undisturbed velocity, the density, and the circulation round a contour enclosing the aerofoil.

‡ Permission to communicate the results was kindly granted by the Aeronautical Research Committee.

§ See § 9 for explanation.

 [Published July 12, 1927.

mathematically and the shape approximates to that of an aerofoil. The position of the stagnation point in the wind tunnel was deduced, for several angles of incidence,* from observations of pressure on the surface of the model. A direct comparison of the two sets of results indicates that the stagnation point for an inviscid flow with an equal circulation† does not, in general, agree in position with that measured in the wind tunnel; and, further, that the distance between the two points increases with the magnitude of the circulation. The differences are such that the circulation for an inviscid flow having a forward stagnation point coincident with that measured in the wind tunnel is smaller than that connected with the measured lift. It is also shown that the measured pressure distribution not only in the immediate vicinity of the stagnation point, but also over a large part of the nose, is more closely represented by theory, when the value of the theoretical circulation taken is that which makes the stagnation points coincide, and not that required to account for the measured lift.

(3) As it is of special interest from an aeronautical standpoint, an analysis similar to that described above has been made for a model aerofoil. It is not possible to estimate the position of the stagnation point for an inviscid flow directly, so recourse was made to the "electrical tank."‡ To determine the accuracy of this method of measurement, a flow pattern for the elliptic cylinder was mapped out in the tank and compared with that deduced by theory (Part II). It was concluded that the general flow pattern could be plotted with fair accuracy, but that estimations of the velocity distribution would probably be unreliable near the aerofoil. The position of the stagnation point for inviscid flow was therefore determined in the electrical tank from the flow pattern at the nose of the aerofoil, but no attempt was made to estimate the pressure distribution in this region.

(4) The analysis for the aerofoil is given in Part III. The wind-tunnel results show that as the angle of incidence increases, the stagnation point travels around the nose towards the under surface; and also that at the critical angle, where there is a sudden fall of lift, there is an abrupt traverse of the stagnation point in the opposite direction. It was found that for the same value of the circulation the stagnation point for an electrical-tank flow did not, in general, agree with that measured in the wind tunnel; and, further, that the displacement between the two points increased with the experimental drag§ of the aerofoil. The differences are such that the circulation for a theoretical flow having a forward stagnation point, coincident with that measured in the wind tunnel, is greater at a low value of the angle of incidence and smaller at a high value than that deduced from the lift measured in the wind tunnel, and the KUTTA–JOUKOWSKI formula. Thus, at zero lift (the angle of incidence $= -8°$ approximately), the stagnation

* Taken as the angle between the major axis and the direction of the undisturbed wind.

† See § 9 for explanation.

‡ This apparatus was designed by Mr. E. F. RELF, and is described in the 'Phil. Mag.,' vol. 48, September, 1924.

§ The theoretical drag is zero.

point is situated on the upper surface, and its position is such that according to theory there is an appreciable lift; this lift is not realised in practice, however, because of the negative pressure in the eddying wake associated with the under surface. On the other hand, at angles of incidence above the critical value, where the lift suddenly falls, the stagnation point is on the under surface, and its position does not differ appreciably from that found for the inviscid flow *without* circulation.

Part I.—Experiments with the Elliptic Cylinder.

(5) The forward stagnation point for a body immersed in a fluid is defined as the point where an approaching stream-line meets the surface at right angles. At this point the velocity in the fluid is zero and, if compressibility can be neglected, the pressure has there a maximum value equal to $\frac{1}{2}\rho V^2$, where V is the velocity of the undisturbed stream. The position of the stagnation point can therefore be determined either from velocity measurements in the approaching stream or, more simply, from observations of pressure taken around the section.

(6) In the present wind-tunnel experiments the stagnation point for a two-dimensional airflow has been taken as the point where the pressure is a maximum, and its position has been determined from pressure observations taken around the median section* of the elliptic cylinder mounted between the walls of a 4-ft. wind tunnel. The major and minor axes of a cross-section of the elliptic cylinder were 5·4 inches and 1 inch respectively. The cylinder was accurately cut from cast aluminium and a large number of holes drilled around the median section. The position of each hole is given in Table I, where x and y are the co-ordinates of a point on the surface, and S represents the peripheral distance from the nose.

Table I shows the spacing of the holes to be such that by taking advantage of the symmetry of the model, and mounting at both positive and negative angles of incidence, a large number of pressure observations can be taken around the nose. By a rotation through 180° the same holes were used to determine the pressure distribution over the rear half of the cylinder. The pressures were measured on a standard 26-inch Chattock gauge. The speed of the wind was 60 feet per second.

(7) The method of experiment was to determine firstly the approximate angle of incidence at which the pressure at each hole was equal to $\frac{1}{2}\rho V^2$. Observations of pressure were then taken as the angle was altered in small steps through this region. The exact incidence at which the pressure was a maximum was then estimated from the curve obtained when the observations of pressure were plotted against angle of incidence.

These pressure curves are given in fig. 1. The results of repeat experiments are included; and these when compared with the original results show that, in general, the angle of incidence which brings the stagnation point to a given position can be determined to an accuracy within $\pm$ 0·3°.

* Earlier experiments have shown that the flow in this region is two-dimensional. *Cf.* "On the Drag of an Aerofoil for Two-Dimensional Flow." By A. Fage and L. J. Jones, 'Roy. Soc. Proc.,' A, vol. 111.

TABLE I.—Unit of Length = One Chord.

Hole.	x.	y.	S.
1	0	0·0925	0·5225
2	0·1665	0·0875	0·3555
3	0·3150	0·0720	0·2065
4	0·4185	0·0510	0·1005
5	0·4690	0·0320	0·0465
6	0·4840	0·0230	0·0285
7	0·4945	0·0140	0·0150
8	0·5000	0·0010	0·0010
9	0·4970	— 0·0100	— 0·0100
10	0·4895	— 0·0195	— 0·0215
11	0·4765	— 0·0280	— 0·0380
12	0·4580	— 0·0370	— 0·0585
13	0·4180	— 0·0510	— 0·1015
14	0·3150	— 0·0720	— 0·2065
15	0·1665	— 0·0875	— 0·3555
16	0	— 0·0926	— 0·5225

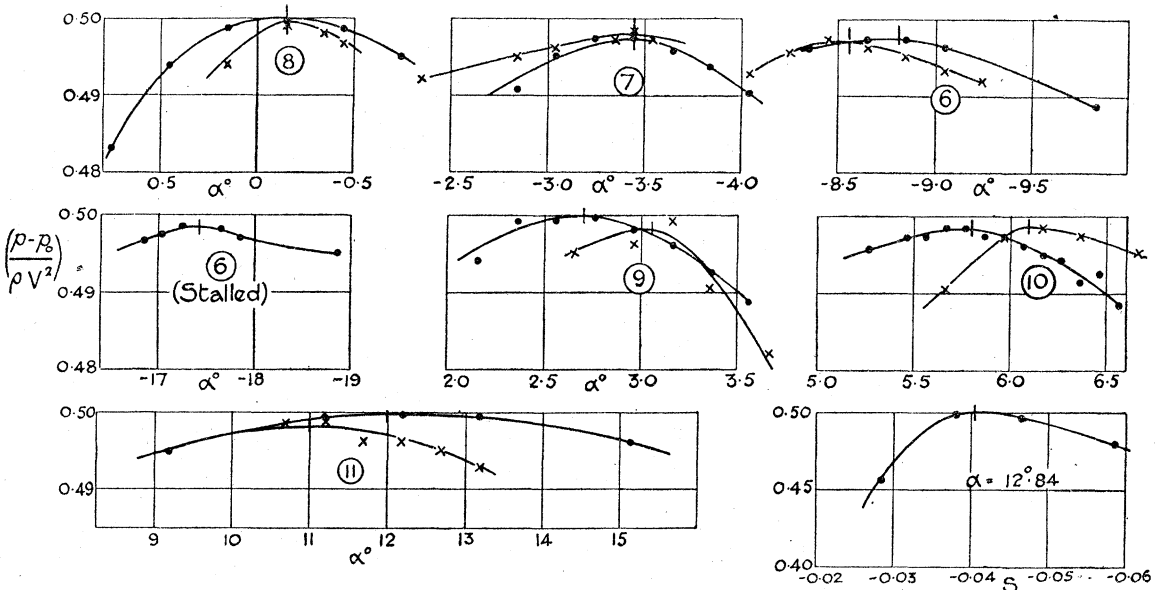

FIG. 1.—Pressure Curves for Elliptic Cylinder. Ringed numbers refer to observation point on section.

(8) The theoretical flow pattern was determined from the general equation given in Lamb's 'Hydrodynamics.'* This equation for a stationary elliptic cylinder, with the major axes inclined at an angle α to an infinite stream moving with unit velocity, is

$$\psi = \Big[-\sqrt{\frac{a+b}{a-b}}\,.\,e^{-\xi}\,(b\sin\eta\,\cos\alpha - a\cos\eta\,\sin\alpha) + \frac{\kappa}{2\pi}\xi + \sqrt{(a^2-b^2)}\,(\cos\alpha\,\sinh\xi\,\sin\eta - \sin\alpha\,\cosh\xi\,\cos\eta)\Big], \quad . \quad . \quad . \quad (1)$$

* See pages 78–86, Fourth Edition.

where

$$x = c \cosh \xi \cos \eta, \quad y = c \sinh \xi \sin \eta \quad \text{and} \quad c = \sqrt{(a^2 - b^2)}.$$

At the surface of the elliptic cylinder $\cos \eta = x/a$ and $\sin \eta = y/b$.

From the above equation it follows, if p be the pressure at any point on the surface, and p_0 the pressure in the undisturbed stream, that

$$\left[1 - 2\frac{(p - p_0)}{\rho}\right]\left[\frac{b^2x^2}{a^2} + \frac{a^2y^2}{b^2}\right] = \left[y \cos \alpha \frac{(a+b)}{b} - x \sin \alpha \left(\frac{a+b}{a}\right) + \frac{\kappa}{2\pi}\right]^2. \quad (2)$$

Further, if (x_0, y_0) be the co-ordinates of the stagnation point, then

$$x_0 \sin \alpha \left(\frac{a+b}{a}\right) - y_0 \cos \alpha \frac{(a+b)}{b} = \frac{\kappa}{2\pi}, \quad . \quad . \quad . \quad . \quad . \quad . \quad . \quad (3)$$

where

$$\frac{x_0^2}{a^2} + \frac{y_0^2}{b^2} = 1.$$

The value of S_0, that is, the peripheral distance of the stagnation point from the nose of the ellipse, was calculated by the use of elliptic functions.

(9) The wind-tunnel travel of the stagnation point with angle of incidence is given by the full line in fig. 2; the points on this line represent values taken from the pressure

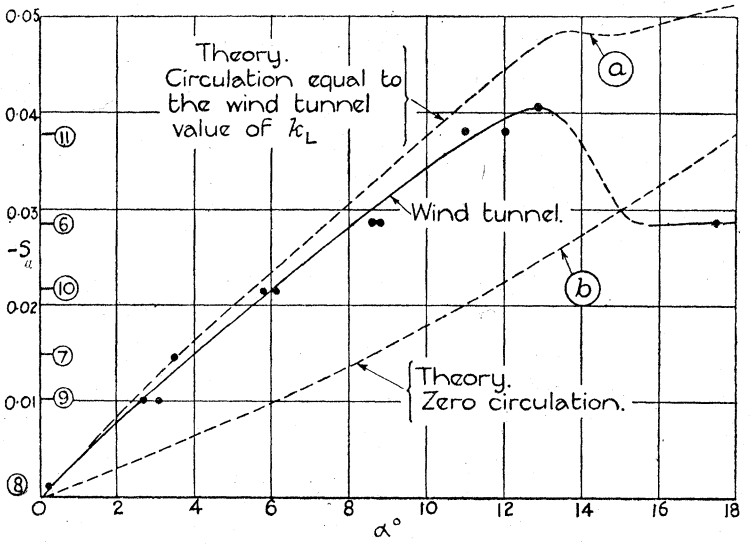

FIG. 2.—Transverse of Stagnation Point with Incidence. Ringed numbers refer to observation point on section.

curves of fig. 1. Included in fig. 2 is a dotted curve which gives the theoretical position of the stagnation point when the circulation (κ) taken is that which would make the theoretical lift equal to that measured in the wind tunnel. According to the theoretical relation of KUTTA and JOUKOWSKI, the magnitude of this circulation is equal to

$$\frac{\text{lift}}{\rho V} = \frac{K_L \rho C V^2}{\rho V} = K_L,$$

since V and C are each taken as unity.

L. W. Bryant and D. H. Williams* have shown, for an angle of incidence below the critical value, that the actual circulation in the wind tunnel is equal to the measured lift coefficient K_L, provided that the contour around which the circulation is measured cuts the wake in a direction more or less at right angles to that of the undisturbed wind, and that it does not approach too closely to the aerofoil. It is to be noted that in the immediate neighbourhood of the aerofoil, the circulation falls very rapidly to zero, since there is no slip at the boundary, whereas with the inviscid flow the magnitude of the circulation remains constant.

Reference to fig. 2 shows that the wind-tunnel observations lie consistently below the theoretical curve (a), and that the discrepancy increases with the angle of incidence. The stagnation point for a flow in the wind tunnel does not agree in position, therefore, with that for a theoretical flow having an equal circulation. Conversely, for the same position of the stagnation point, the value of the circulation (K_L) for a theoretical flow differs from the value related (in the manner explained above) to the wind-tunnel lift. This comparison is given in Table II, and shows that the theoretical values of K_L are smaller than those measured in the wind-tunnel and that the difference increases with the angle of incidence. The wind-tunnel values of K_L were estimated from the measured pressure distribution around the section; the theoretical values of K_L were calculated from equation (3) above.

Table II.—Values of K_L.

Angle of Incidence. $\alpha°$	Common stagnation point.		
	Wind tunnel.	Theory.	Difference.
2·70	0·260	0·225	0·035
3·05	0·285	0·200	0·085
3·45	0·310	0·335	— 0·025
5·80	0·410	0·395	0·015
6·10	0·420	0·385	0·035
8·55	0·470	0·385	0·085
8·80	0·475	0·370	0·105
11·00	0·495	0·435	0·060
12·00	0·495	0·370	0·125
12·85	0·495	0·370	0·125
Above the critical angle 14·85	0·384	—	—
Above the critical angle 17·45	0·277	— 0·198	0·475

(10) Further evidence in support of the conclusions drawn in § 9 were obtained from comparisons between the theoretical and wind-tunnel distributions of pressure around the nose. These comparisons have been made for three angles of incidences, at 8·84°, 12·84° and 17·45°; that is, below, at, and above the critical angle respectively. At each angle of incidence, the pressure distribution has been determined from equation

* *Loc. cit.*, § 1.

(2), § 8, for two theoretical flows which are related to the wind-tunnel flow in such a manner that in one case the stagnation points coincide in position, and in the other the circulations are the same. These theoretical results, together with the values measured in the wind tunnel, are plotted in figs. 3–5. These curves show that, in general, the measured

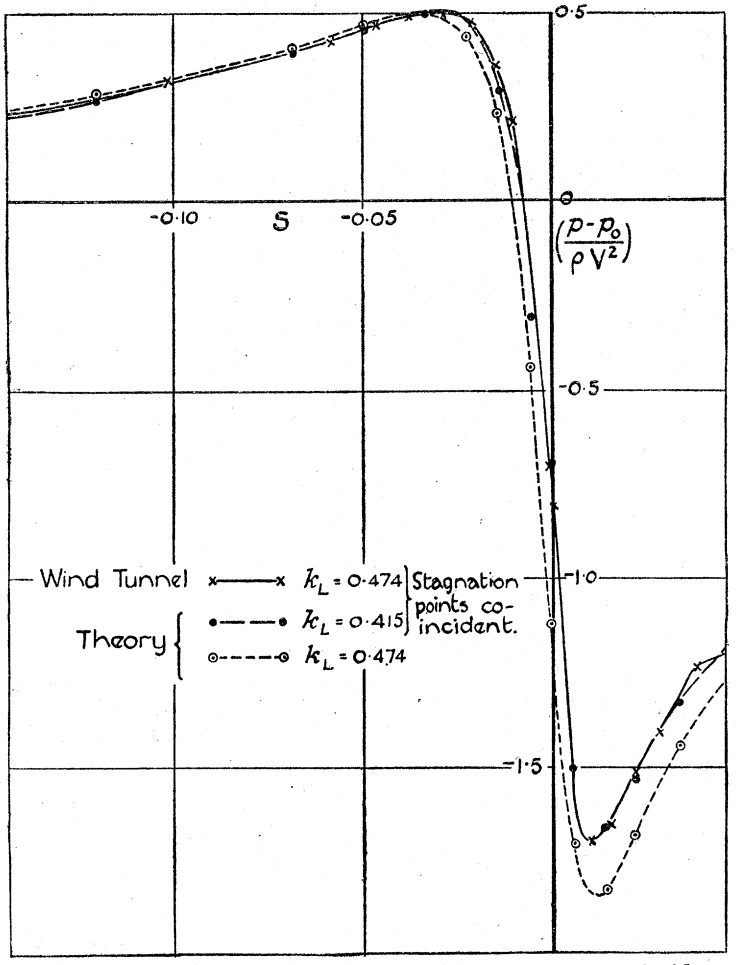

FIG. 3.—Pressure Distribution around Nose of Elliptic Cylinder. Incidence 8·84°.

pressure distribution not only in the immediate region of the stagnation point, but also over a large part of the nose, is more closely represented by theory, when the value of the circulation taken is that which makes the stagnation points coincide. The actual value of this circulation—given on the appropriate curve in each figure—is seen to be smaller than that for the circulation related to the measured lift. The comparison given in fig. 5 for the flow beyond the critical angle is of special interest. In this case, the actual flow at the nose—up to the point $S = 0$, where the dead-air region commences—is almost the same as that for a theoretical flow having an appreciable negative circulation (—0·198).

(11) As a matter of general interest, two comparisons between the theoretical and wind-tunnel distributions of pressure around the entire periphery of a cross-section of

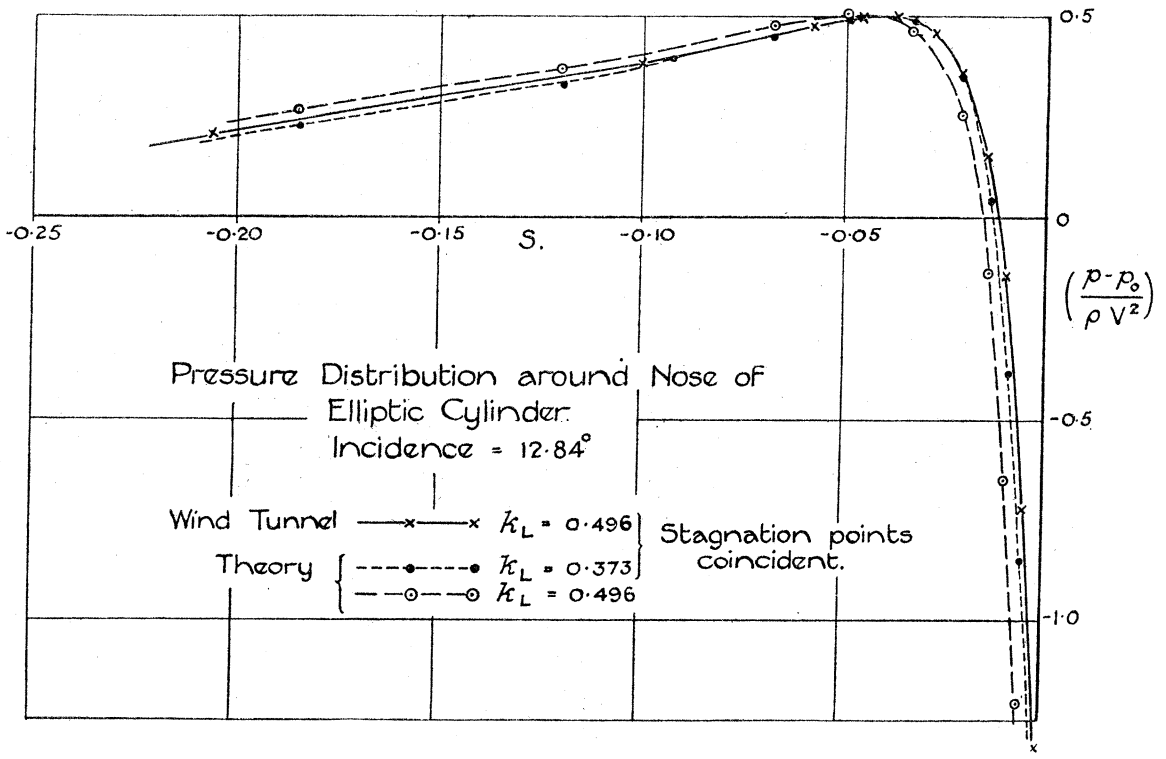

FIG. 4.

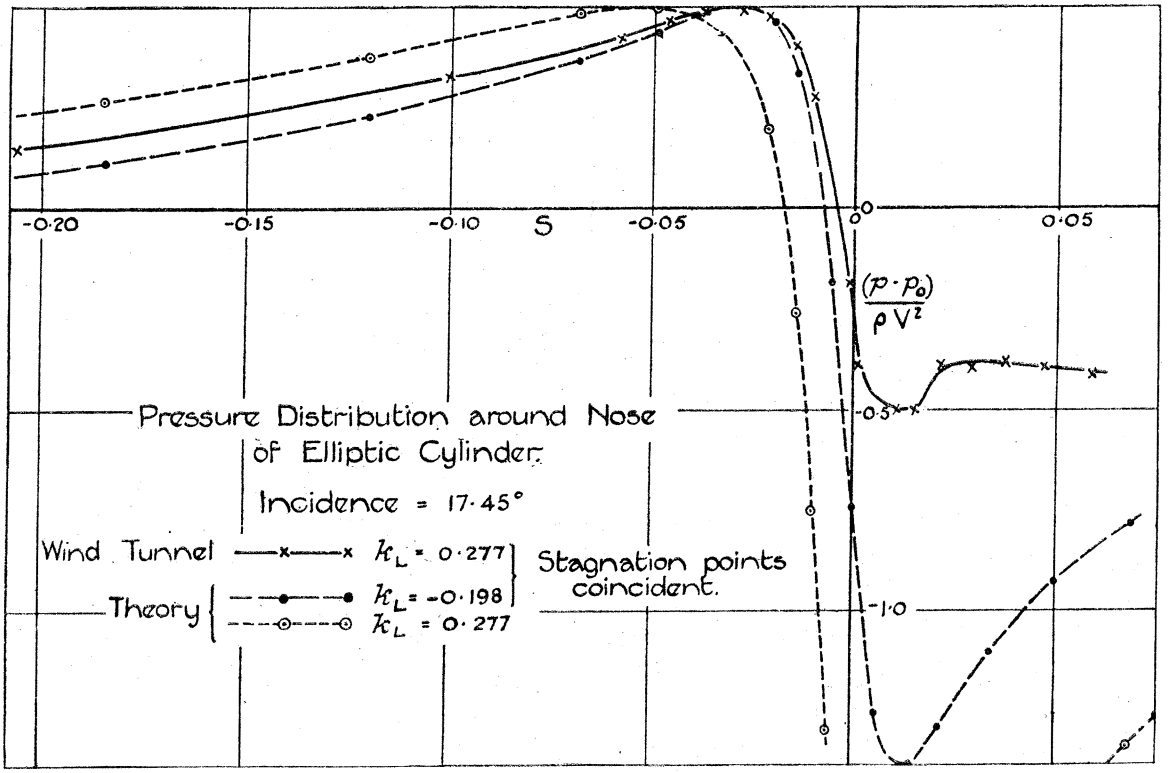

FIG. 5.

the elliptic cylinder are included in the paper. The first comparison, given in fig. 6, shows that, at 0° angle of incidence, theory and experiment are in close agreement for

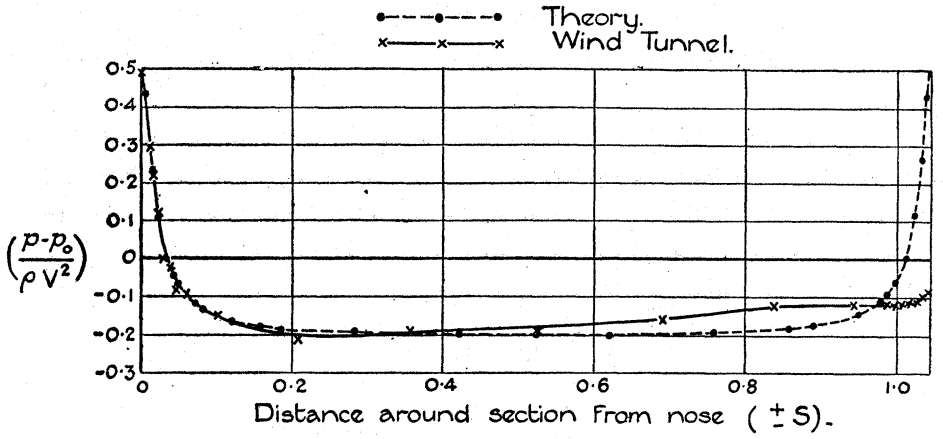

FIG. 6.—Elliptic Cylinder. 0° Incidence.

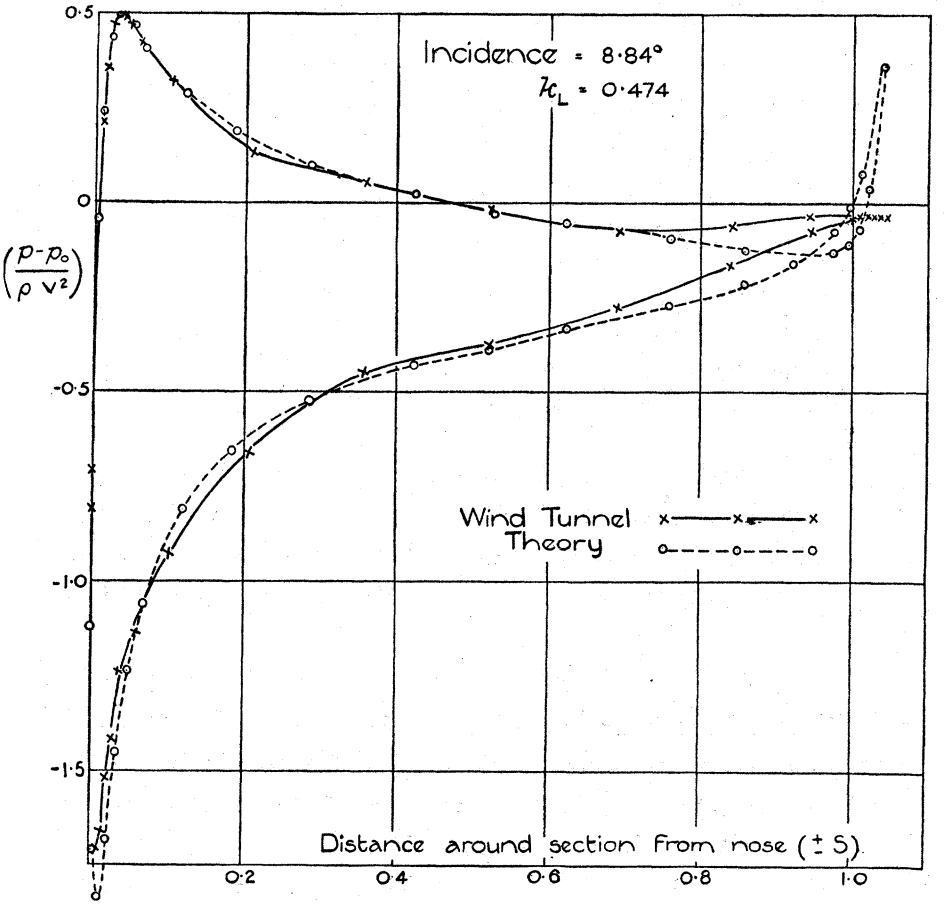

FIG. 7.—Elliptic Cylinder.

the forward half of the model. The wind-tunnel curve then remains at a more or less steady negative value, whereas the theoretical pressure increases and finally has a value $+\frac{1}{2}\rho V^2$ at the tail. The second comparison, fig. 7, is for an angle of incidence of

$8 \cdot 84°$ and $K_L = 0 \cdot 474$. As in the previous case, the agreement is fairly close over the forward half of the model. The discrepancy between theory and experiment is, however, very marked over the after portion, owing to the presence of the wake. It is shown in fig. 3 that a closer agreement at the nose can be obtained for a theoretical circulation of value $0 \cdot 415$.

(12) Although not directly connected with the subject matter of the paper, it is desired to place on record that it was found that at a small angle of incidence about 35 per cent. of the drag of the elliptic cylinder arose directly from the tangential forces at the surface. The method of measurement was the same as that described in an earlier paper.* The actual results are given in Table III.

TABLE III.

Angle of incidence. $\alpha°$	Total drag coefficient. From total-head measurement. (A)	Drag coefficient from integration of pressure observations.	Drag due to tangential forces. (B)	$\frac{(B)}{(A)}$
$0 \cdot 16$	(*b*) $0 \cdot 0225$, (*b*) $0 \cdot 0209$, (*a*) $0 \cdot 0206$ } $0 \cdot 0213$	$0 \cdot 0148$	$0 \cdot 0065$	$0 \cdot 31$
$0 \cdot 84$	(*a*) $0 \cdot 0207$, (*b*) $0 \cdot 0222$ } $0 \cdot 0214$	$0 \cdot 0134$	$0 \cdot 0080$	$0 \cdot 37$
$2 \cdot 84$	(*a*) $0 \cdot 0160$, (*b*) $0 \cdot 0158$ } $0 \cdot 0159$	$0 \cdot 0100$	$0 \cdot 0059$	$0 \cdot 37$
	(*a*) 6 in. behind trailing edge. (*b*) 12 in. behind trailing edge.			

It should be noted that the drag of the elliptic cylinder at an angle of incidence of $2 \cdot 84°$ is appreciably lower than that at 0°. The drag coefficient due to the tangential forces for the aerofoil used in the experiments of Part III was found to be about $0 \cdot 0030$ in the region of minimum drag, that is, about 20 per cent. of the total drag.

PART II.—THE ACCURACY OF THE ELECTRICAL TANK.

(13) The position of the stagnation point for an inviscid flow around the aerofoil has been determined indirectly in the electrical tank,† in view of the fact that a direct determination was not possible. To establish the value of this work (given in Part III) an investigation was undertaken to determine, firstly, how closely the flow mapped out in the electrical tank resembled the flow of an inviscid fluid, especially in the region of the stagnation point, and, secondly, whether it was possible to estimate from the flow pattern the pressure distribution around the surface. This investigation will now be described.

* *Loc. cit.*, § 6.

† *Loc. cit.*, § 3.

(14) The method of the electrical tank depends on the fact that the stream-lines for an inviscid flow and the equi-potential lines in an electrical field are identical when the boundary conditions correspond. Apart from minor modifications introduced to improve the accuracy of measurement, the general scheme followed in the present experiments was the same as that described in the paper by L. W. Bryant and D. H. Williams.* Two sets of diagrams were taken, first that of the stream-lines without circulation, and second that of the stream-lines for circulation alone. The flow pattern with circulation was obtained by the superposition of the two diagrams.

The experiments were made on the elliptic cylinder used in Part I, a form for which the solution of the equation $\nabla^2\psi = 0$ is known. The flow pattern was measured in the tank with the cylinder at an incidence of 10° and for an assumed circulation of 0·7. To allow a rigid comparison with the theoretical flow pattern for an infinite stream, account should be taken of the effect of the walls of the electrical tank. No exact method of estimating the magnitude of this correction appears to be possible—since the boundary conditions at the ellipse as well as at the walls have to be satisfied—but an approximate method based on an infinite series of images, which neglected the boundary conditions at the ellipse, showed the correction to be very small. This is to be expected since the size of the ellipse is small compared with the dimensions of the tank (60 inches by 27 inches), and the exploration was limited to a narrow region close to the surface.

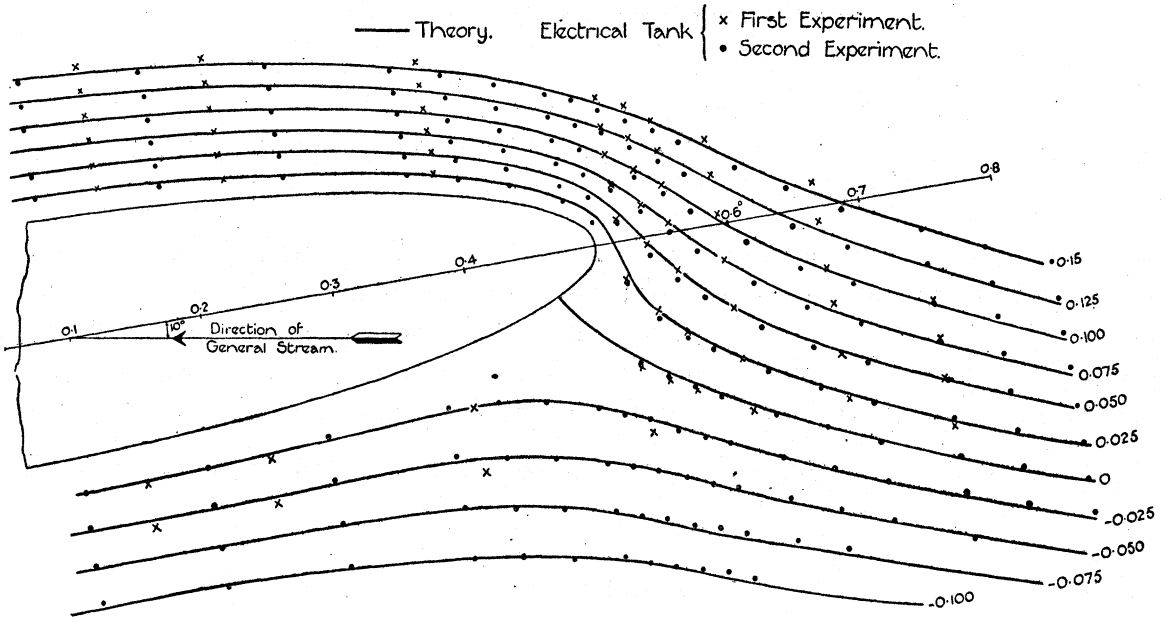

Fig. 8.—Incidence 10°. Circulation 0·7.

(15) The theoretical stream-lines for an infinite stream were calculated from equation (1) of § 8, and are given by the full lines in fig. 8. Included on the diagram are points representing the results obtained from two independent plottings in the electrical tank. The points are seen to be fairly close to the full lines, but there appears in each

* *Loc. cit.*, § 1.

experiment a small but consistent difference from theory. The sign of this discrepancy differs in the two experiments. The uncertainty in the position of the zero stream-line does not appear to be large, and, in this particular test, results in a possible error of 0·02 inch (0·004 chord) in the position of the stagnation point. The conclusion drawn from the comparison is that the electrical tank in its present form maps out the general flow with fair accuracy.

(16) The velocity at any point on the surface can be found from the slope of the curve obtained when the stream-function ψ is plotted against the normal distance from the surface. A representative curve for the region of high velocity at the nose is given in fig. 9. It is seen that the two series of values estimated from the electrical-

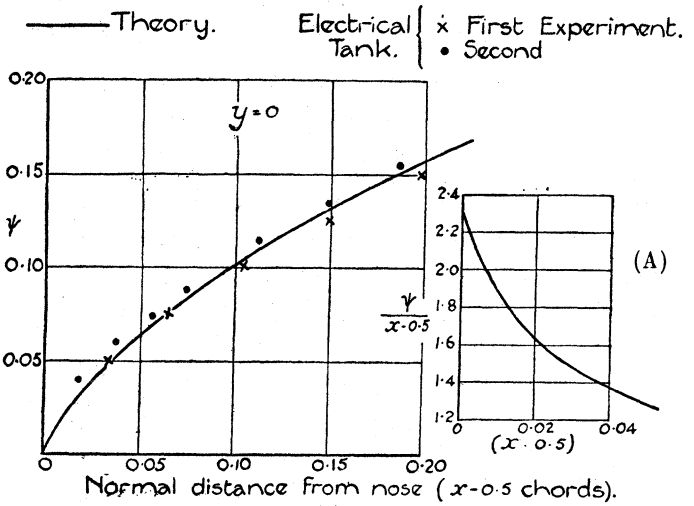

Fig. 9.—Elliptic Cylinder. Circulation 0·7. Incidence 10°.

tank results lie on opposite sides of the theoretical curve. The average displacements from the theoretical curve are $\pm$ 0·006 chord ; and the error on velocity due to this inaccuracy of observation is of the order of $\pm$ 8 per cent. A more serious cause of error probably arises, however, from the uncertainty in the measurement of the rapid change of ψ in the immediate neighbourhood of the surface. This is illustrated in fig. 9 (A), where theoretical values of $\left(\frac{\psi}{x - 0{\cdot}5}\right)$ are plotted against x. The velocity at the surface is, of course,

$$\operatorname*{Lt}_{x \to 0{\cdot}5} \left(\frac{\psi}{x - 0{\cdot}5}\right),$$

and is equal to 2·31. The values of $\left(\frac{\psi}{x - 0{\cdot}5}\right)$ at $x = 0{\cdot}004$ chord is 2·09, that is, 90 per cent. of the true velocity. The inaccuracy in the estimated value of the velocity may, therefore, exceed 10 per cent., unless the value of ψ can be measured within 0·02 inch from the surface. It follows, then, that good accuracy in the measurement of velocity at the nose can only be obtained when the gradient of ψ is measured very close to the

surface. Fig. 10 shows that at the flat part of the ellipse (taken at $x = 0{\cdot}2$ chord) there is an almost linear variation of ψ with y (that is, normal distance approximately), and that the velocity can be measured within an accuracy of $\pm$ 4 per cent. The general

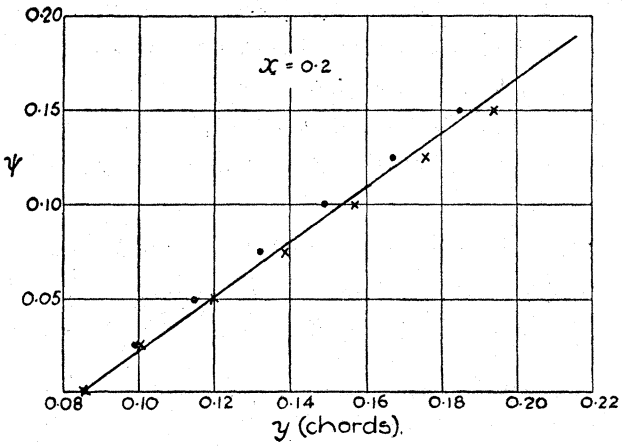

FIG. 10.

conclusion to be drawn from the above discussion is that the velocity distribution will probably not be determined with good accuracy with the present method of measurement.

PART III.—EXPERIMENTS WITH THE AEROFOIL.

(17) The aerofoil (6-inch chord) was mounted between the walls of a 4-foot tunnel, and measurements of pressure taken around the median section, at several angles of incidence. The general shape of the section is given at the top right-hand corner of fig. 11. The large-scale sketch included at the bottom left-hand corner shows the

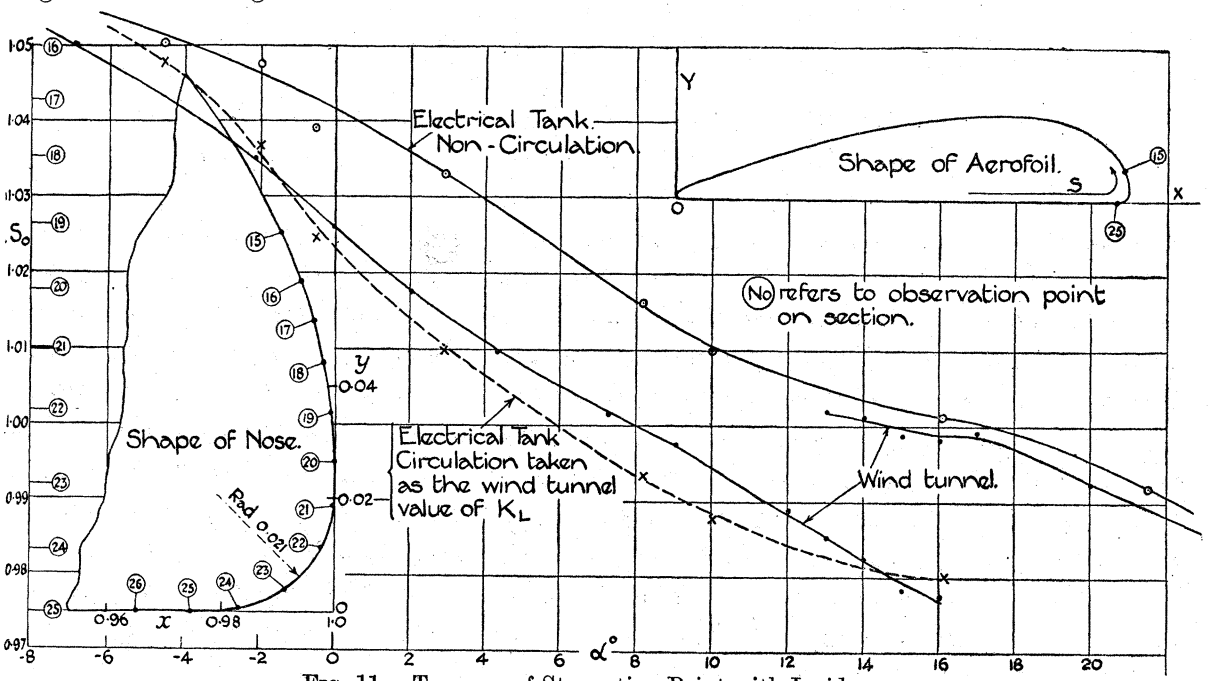

FIG. 11.—Traverse of Stagnation Point with Incidence.

shape of the nose and also the positions of the pressure holes. The central part of the aerofoil was accurately cut from cast aluminium, and a large number of holes were drilled in the nose. A close spacing of the holes was obtained by staggering them in three transverse rows, the two outer rows being about 0·02 chord from the median section. The spacing in each of these rows was about 0·024 chord, so that the average distance between the pressure observations was 0·008 chord. The pressure was measured on a standard 26-inch Chattock gauge. The speed of the wind was 60 ft.-sec. The angle of incidence, α, has been taken as the angle between the chord and the undisturbed wind direction.

No detailed description of these wind-tunnel experiments is needed, as the general procedure followed was the same as that for the elliptic cylinder (Part I, § 7). The pressure curves shown in fig. 12 give the angle of incidence at which each observation

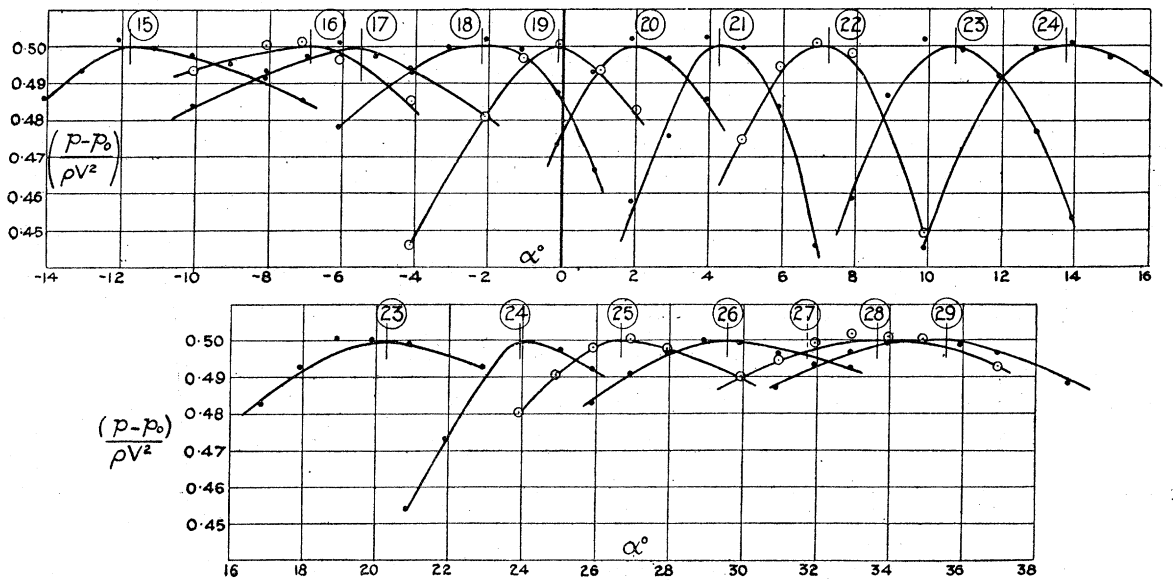

FIG. 12.—Pressure Curves. Ringed numbers refer to observation point on section.

hole becomes a stagnation point. It is there seen that the angle of incidence which brings the stagnation point to a given position can be determined to an accuracy within $\pm 0{\cdot}3°$. Reference to fig. 11 shows that the corresponding uncertainty in the measurement of the position of the stagnation point is small, and amounts to about 0·0008 chord. The final results are collected in Tables IV and IVA. The values of the co-ordinates (x, y) of a point, and the peripheral distance S_0, measured from the trailing edge in an anti-clockwise direction, are there given in terms of the chord to the nearest 0·0005. The position of the axes OX and OY are given in fig. 11. The values in Table IVA were obtained by plotting the pressure results against S at a constant angle of incidence.

(18) The values of S_0 given in Tables IV and IVA are plotted against the corresponding values of the angle of incidence in fig. 11. The curves drawn through these points show clearly the traverse of the stagnation point with angle of incidence. As

the angle of incidence increases, the stagnation point moves around the nose towards the under surface at a fairly uniform rate, until the critical angle is reached, at which

TABLE IV.

Point on section.	x	y	S_0	Incidence at which the pressure at point is equal to $\frac{1}{2}\rho V^2$. α degrees.
10	0·9665	0·1030	1·1025	—
11	0·9730	0·0950	1·0920	—
12	0·9780	0·0890	1·0845	—
13	0·9820	0·0820	1·0765	—
14	0·9865	0·0745	1·0675	—
15	0·9905	0·0670	1·0590	— 11·8
16	0·9940	0·0585	1·0500	— 6·9
17	0·9960	0·0515	1·0430	— 5·5
18	0·9980	0·0440	1·0350	— 2·2
19	0·9995	0·0355	1·0260	— 0·1
20	1·0000	0·0270	1·0175	2·0
21	1·0000	0·0190	1·0100	4·25
22	0·9975	0·0115	1·0020	7·20
23	0·9910	0·0040	0·9920	10·7 and 20·25
24	0·9830	0·0005	0·9830	13·7 and 23·9
25	0·9750	0	0·9750	26·65
26	0·9650	0	0·9650	29·55
27	0·9565	0	0·9565	31·70
28	0·9485	0	0·9485	33·65
29	0·9400	0	0·9400	35·50
30	0·9320	0	0·9320	—
31	0·9260	0	0·9260	—
32	0·9120	0	0·9190	—
33	0·9090	0	0·9090	—

TABLE IVA.

Angle of incidence. Degrees.	Value of S_0.
14·0	0·9825 1·0015
15·0	0·9785 0·9990
16·0	0·9775 0·9985
17·0	0·9990

the flow suddenly breaks down. The stagnation point then has an abrupt shift in the opposite direction, but afterwards continues to travel in the same direction as

formerly, although at a slower rate. It will be observed in fig. 11 that the lower part of the nose is a quadrant of a circle of small radius (0·021 chord). When the flow breaks down, the stagnation point traverses practically the whole length of this quadrant; that is, the zero stream-line, which is at right angles to the aerofoil surface at the stagnation point, turns through almost 90°. It is also seen that two distinct positions of the stagnation point have been measured in the critical region, that is, between $\alpha = 13°$ and $\alpha = 16°$.

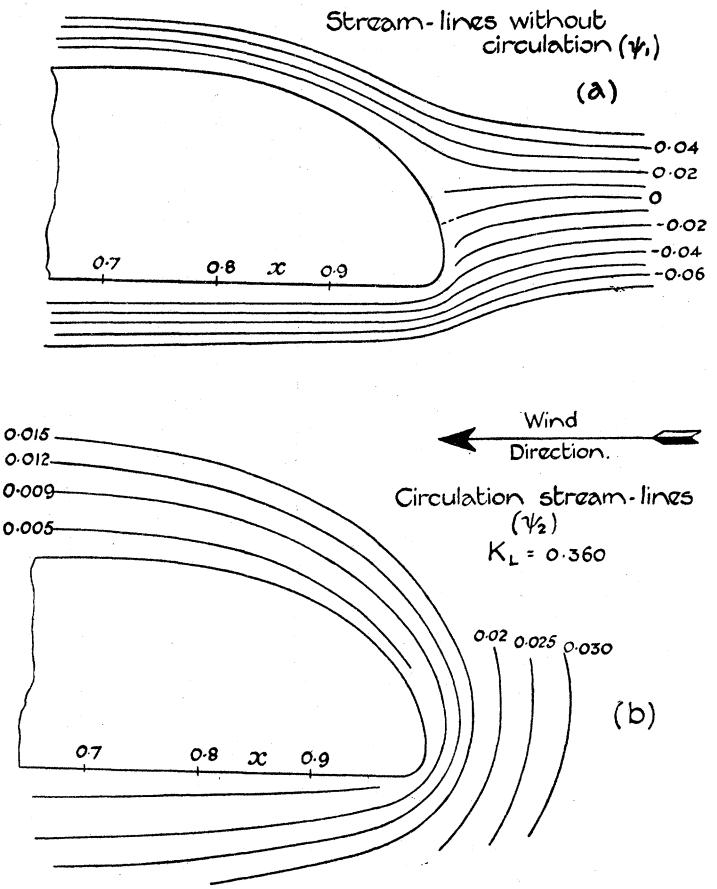

FIG. 13.—Stream-lines for —2° Incidence.

(19) As previously mentioned, the position of the stagnation point for an inviscid flow was inferred from the flow pattern measured in the electrical tank. The aerofoil used in these experiments was cut from cast aluminium at the same time as the central part of the aerofoil used in the wind tunnel. The two sections are therefore identical.

The stream-lines for the flow without circulation were traced with the aerofoil at angles of incidence of — 4·55°, — 2·0°, — 0·55°, 2·90°, 8·15°, 10°, 16·1° and 21·5°. The general character of these diagrams is illustrated in fig. 13 (*a*), where the actual stream-lines traced out when the aerofoil was at — 2° are reproduced. No attempt has been made to explore within a distance of 0·015 chord (approx.) from the aerofoil surface—because the accuracy of measurement within this region was unsatisfactory.

The stream-line system for circulation alone was also traced out with the aerofoil at several angles of incidence. These flow systems were found to be identical in the neighbourhood of the aerofoil, within the accuracy of experiment. The value of the stream-function (ψ_2) at any point in this field is proportional to the circulation. A representative tracing of a flow pattern of this type, which shows the general spacing of the stream-lines, is given in fig. 13 (*b*); the figures on the curves refer to a circulation of 0·360.

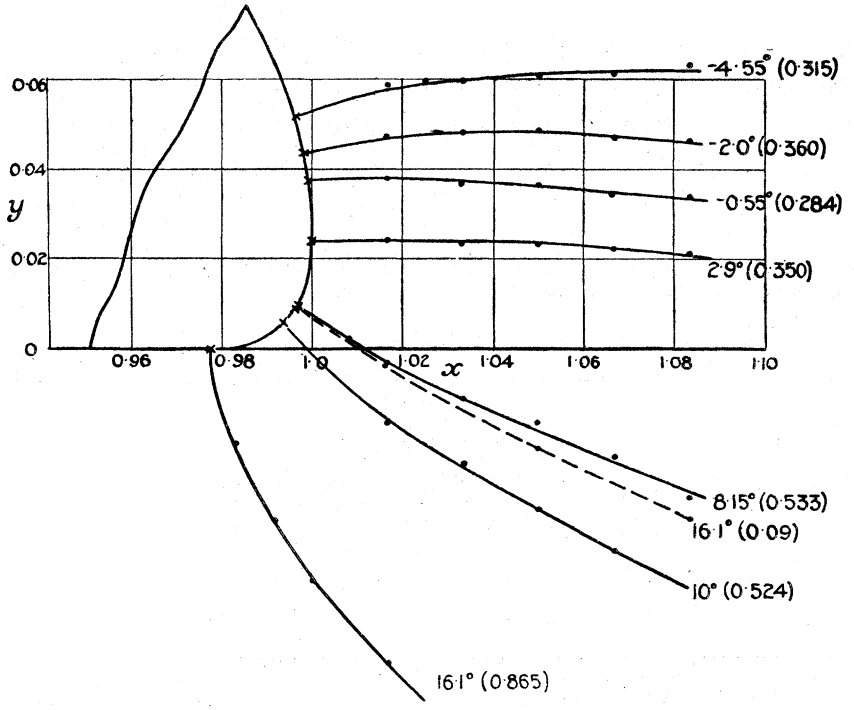

FIG. 14.—Zero Stream-lines. Values of Circulation given in Brackets. ● Electrical Tank Results. × Wind Tunnel Results.

(20) The position of a stagnation point for a flow without circulation was determined by re-plotting the traced part of the stream-line ($\psi_1 = 0$) on as large a scale as was consistent with the experimental accuracy, and then producing this line to meet the aerofoil surface at right angles. This method was adopted because a direct measurement of the position could not be made. These results are given in Col. (*c*), Table V.

The position of the stagnation point for a flow with circulation was obtained in the same way, that is, by drawing the zero stream-line ($\psi_1 + \psi_2 = 0$) through the points estimated from the electrical-tank results. Representative stream-lines of this type are given in fig. 14 (see later, § 22). The points on these lines represent actual values estimated from the electrical tank. Reference to this figure shows that the stream-lines were plotted in the tank to a distance of 0·015 chord from the nose. The shape near the aerofoil was then determined from the fact that each line must meet the surface at right angles. It was found by trial that there is very little latitude when fixing the shape of a stream-line at the aerofoil surface, and that uncertainties in the

position of the stagnation point due to this cause should not, in general, exceed $\pm$ 0·0007 chord.

(21) The first series of calculations was made to determine the position of the stagnation point for an electrical-tank flow having a circulation equal in magnitude to that related to the wind-tunnel lift. The value of this circulation has been taken as the wind-tunnel value of the lift coefficient K_L. (See elliptic cylinder § 9.) These calculated values of S_0 are given in Col. (*d*), Table V. They are plotted against α (dotted line) in fig. 11 to allow a comparison with the wind-tunnel results. Except in the neighbourhood of —1° the two curves are not in agreement. Further, since the differences are greater than the probable experimental inaccuracies, it is concluded that the stagnation point, estimated from observations taken in the electrical tank, for a theoretical flow with an equal circulation does not, in general, agree in position with that measured in the wind tunnel.

TABLE V.—The value of S_0 gives the position of the stagnation point. (See also fig. 11.)

Angle of incidence. α°.	Wind tunnel.		Electrical tank.			Col. (*b*) — Col. (*e*).	Wind tunnel.
	S_0.	K_L.	Value of S_0 when $K_L = 0$.	Value of S_0 for K_L measured in wind tunnel.	Value of K_L for the value of S_0 measured in the wind tunnel.		K_D.
	(*a*)	(*b*)	(*c*)	(*d*)	(*e*)	(*f*)	(*g*)
—8·0	1·0525	0·035	1·0570	1·0565	—	—	0·0505
—4·55	1·0425	0·162	1·0505	1·0480	0·315	—0·153	0·0255
—2·0	1·0345	0·290	1·0475	1·0370	0·360	—0·070	0·0160
—0·55	1·0285	0·355	1·0390	1·0248	0·284	+0·071	0·0140
+2·90	1·0145	0·516	1·0330	1·0100	0·350	0·166	0·0135
8·15	0·9990	0·707	1·0160	0·9935	0·533	0·174	0·0180
10·0	0·9940	0·760	1·0100	0·9875	0·524	0·236	0·0210
14·0	0·9825	0·810	1·0035	0·9815	0·730	0·080	0·0310
*	1·0015	0·395	1·0035	—	0·115	0·280	—
* 16·1	0·9775	0·810	1·0015	0·9800	0·865	—0·055	—
*	0·9990	0·400	1·0015	0·9925	0·090	+0·310	—
18·0	0·9970	0·415	0·9990	—	0·070	0·345	—
21·5	0·9890	0·450	0·9915	0·9600	0·030	0·420	—

* Critical region.

(22) A second series of calculations was then made to determine the strength of the circulation which makes the theoretical position of the stagnation point coincide with that measured in the wind tunnel. These results are given in Col. (*e*), Table V. The zero stream-lines for these flows are given in fig. 14, where the points represent the values estimated from the electrical-tank results and the crosses the wind-tunnel positions

of the stagnation point. It will be seen that very little uncertainty appears to exist as to the shape of these stream-lines. The differences between the wind-tunnel and electrical-tank values of K_L are given in Col. (f), Table V; they are seen to be large, especially at extreme angles of incidence, both positive and negative. There is, however, close agreement in the region between $\alpha = -0{\cdot}55°$ and $\alpha = 2{\cdot}90°$, that is, when the drag is small. [See Col. (g).]

(23) An attempt will now be made to show that the differences given in Col. (f), Table V, can be associated, in a general manner, with the differences between the wind-tunnel and the theoretical flows around the aerofoil. Earlier wind-tunnel experiments* on the measurement of the total-head losses in the wake of this aerofoil have shown, at an incidence of $-6°$, that the air soon after passing the nose breaks away from the under surface, and that a large part of the drag arises from a band of low pressure caused thereby. This pressure acts on a flat under surface, and so is equivalent, in so far as the forces on the aerofoil are concerned, to a downward normal force of magnitude approximately equal to $K_D \rho A V^2$ cosec 6°, where K_D is taken to be the measured drag coefficient. The lift component of this force is $-K_D \rho A V^2$ cot 6°, that is, 0·329, since $K_D = 0{\cdot}0345$. If, then, this "wake" effect be superimposed on the lift calculated from the experimental position of the stagnation point, the lift coefficient would be considerably reduced (from 0·295 to $-0{\cdot}034$), and at the same time brought into much closer agreement with the measured value (0·085). A still closer agreement would be obtained if allowance could be made for the small part of the wake which is associated with the upper surface. The close agreement on lift obtained in the region of minimum drag is not unexpected, because the wake is then narrow and related, more or less equally, to both the upper and lower surfaces, so that its effect on lift should be small. As the incidence increases, the wake becomes wider and arises largely from the flow over the upper surface, and so makes positive contribution to the lift—that is, the experimental lift should be greater than the theoretical value. This is seen to be the case except in the region of the critical angle, where apparently the argument does not hold. Above this angle of incidence the flow abruptly breaks down, and calculations for a stream-line flow are, obviously, precarious. They have been made, however, and show that the theoretical lift is very small, or, in other words, that the motion of air in the region of the stagnation point (now situated on the under surface) closely resembles that for a theoretical flow *without* circulation—a result not unexpected, since in practice there is a wide band of negative pressure above the upper surface, which probably accounts for a large part of the lift.

(24) In conclusion, the writer wishes to express his gratitude to Prof. L. Bairstow and to Dr. H. Lamb for valuable advice given during the preparation of the paper.

* *Loc. cit.*, § 6.

PHILOSOPHICAL TRANSACTIONS OF THE ROYAL SOCIETY A MATHEMATICAL, PHYSICAL & ENGINEERING SCIENCES